# THEORETICAL AND PRACTICAL INVESTIGATIONS ON THE DETERMINATION OF CALCIUM SILICATE AND AUTOCLAVED AERATED CONCRETE MASONRY COMPRESSIVE STRENGTH

M. GRAUBOHM
Dipl.-Ing., Research assistant in the working group "masonry"
Institute of Building Materials Research (ibac), RWTH Aachen University, Germany

H. ZACHERT
Dipl.-Ing., Former student assistant in the working group "masonry"
Institute of Building Materials Research (ibac), RWTH Aachen University, Germany

W. BRAMESHUBER
Prof. Dr.-Ing., Professor and Director
Institute of Building Materials Research (ibac), RWTH Aachen University, Germany

## SUMMARY

In this paper the results of extensive theoretical (Finite Element Method) and experimental investigations on the determination of the compressive strength of masonry pillars of solid calcium silicate and autoclaved aerated concrete units are presented.

## INTRODUCTION AND STATE OF THE ART

Fundamental investigations by Hilsdorf (1965) regarding the load bearing and fracture mechanisms of masonry under compressive load showed that the masonry strength does not only depend on the strength of the single components but, amongst others, also on their different deformation behaviours. Thus, the load bearing behaviour of masonry under vertical compressive load is considerably influenced by the different material properties of its components, especially by the horizontal deformation differences between masonry units and masonry mortar. As a rule, the mortar experiences a substantially higher lateral strain than the masonry unit which is, however, obstructed by the bond between unit and mortar. The obstruction of the lateral expansion of the mortar by the masonry unit results in additional compressive stresses in the mortar and tensile stresses in the masonry unit normal to the load direction. This entails a triaxial state of stress in the masonry unit which can decrease the masonry strength depending on the height of the lateral tensile stresses in the unit and the lateral deformability of the mortar. Therefore the compressive failure of the masonry mostly occurs when the lateral tensile strength of the masonry units is exceeded.

A purely theory-based and confirmed solution to calculate the masonry compressive strength considering the essential influence parameters has so far not been available despite numerous investigations concerning this subject. In the current European regulations, the masonry compressive strength is therefore at present only approximately determined on the basis of

test results with the following empirical equation by Mann (1983) subject to the uniaxial compressive strength values of the single components, unit and mortar:

$$f_k = K \cdot f_b^{\alpha} \cdot f_m^{\beta} \quad (1)$$

$f_k$ characteristic compressive strength of the masonry in N/mm²
$f_b$ compressive strength of the unit in N/mm², tested on units according to the respective German product standards
$f_m$ compressive strength of the mortar in N/mm², tested on prisms according to DIN EN 1015-11
K, $\alpha$, $\beta$ parameters

Here, the constant K to be placed in the given equation as well as the exponents $\alpha$ and $\beta$ are parameters which are stated depending on the respective masonry unit – masonry mortar combination. In doing so, at the mortar compressive strength exponentiated with the exponent $\beta$, the compressive strength of the mortar determined according to the mortar standard is normally inserted although, as expected, the accuracy of the approximation is higher when the compressive strength of the mortar determined in the joint is applied, cf. Metje (1983).

The aspect to be considered in this connection concerns the water content in the mortar joint depending on the interaction between the water absorption behaviour of the masonry unit and the water retaining capacity of the mortar and that considerably influences the hardening mechanism as well as the strength of the mortar in the joint. In Riechers (2000), for the first time a model is described by which the influence of the water content in the joint on the structure of the fresh mortar and on the hydration processes can be explained.

The previously described influences make it quite clear that the determination of the masonry compressive strength only on the basis of the uniaxial compressive strength values of masonry unit and mortar inevitably has to entail deviations from the actual strength. Extensive theoretical and experimental investigations were carried out with the aim to correctly describe in a numerical model the load bearing behaviour of masonry under vertical compressive stress considering all influencing factors. First steps are described in this contribution.

## TEST PROGRAMME AND APPLIED MATERIALS

Calcium silicate masonry units (CS) and autoclaved aerated concrete units (AAC) with the standard size of (240 · 115 · 71 mm³) were applied. For this purpose the autoclaved aerated concrete specimens had to be sawn from blocks (499 · 365 · 249 mm³) as autoclaved aerated concrete units are normally not produced in this particular size. As masonry mortars, two general purpose mortars of different strength classes (mortar class M2.5 and M10) were used. Numerous compressive tests on 9-unit pillars were conducted with these materials. In doing so, besides the masonry unit type and the mortar class, also the joint thickness (12 mm and 18 mm) was varied which led to the combinations stated in Table 1. In addition, all essential mechanical properties of the applied materials were determined as input parameters for the numerical simulations conducted in parallel.

Table 1. Test programme (masonry pillars)

| Test series | Unit type | Mortar type | Joint thickness [mm] | Number of specimens |
|---|---|---|---|---|
| CS-M2.5-12 (CI) | CS | M2.5 | 12 | 6 |
| CS-M2.5-18 (CII) | | | 18 | 6 |
| CS-M10-12 (CIII) | | M10 | 12 | 6 |
| CS-M10-18 (CIV) | | | 18 | 6 |
| AAC-M2.5-12 (AI) | AAC | M2.5 | 12 | 6 |
| AAC-M2.5-18 (AII) | | | 18 | 6 |

Here, the applied materials and parameters were chosen in a way that different types of failure were to be expected because of the different ratios between the strength, stiffness and lateral strain of unit and mortar and because of the two joint thicknesses. The autoclaved aerated concrete pillars were manufactured exclusively in combination with the mortar M2.5, as the mortar class M10 has a considerably higher compressive strength than the applied autoclaved aerated concrete units. A combination of AAC with M10 would cause a failure basically different from that of the unit-mortar combinations usually applied in practice and was therefore not examined.

## PROPERTIES OF THE UNIT MATERIAL

### Compression tests on cylinders

To determine the compressive strength and the stress-strain relationship of the applied materials, investigations on cylinders (CS: ∅ = 50 mm, l = 100 mm; AAC: ∅ = 100 mm, l = 200 mm) were carried out. For this purpose, cylinders had to be drilled from the calcium silicate units in longitudinal direction because it was impossible to drill a core with a sufficient slenderness in the direction of the unit height due to the small size of the units. To be able to quantify a possible directional influence on the determined compressive strength, in addition to the cylinders also two cubes were taken from each unit and tested in direction of the unit height and length. In the process, a dependency on the direction of the compressive strength could not be discerned. For the small-specimen tests on the autoclaved aerated concrete, the cylinders could be taken from the blocks in the direction of the unit height.

On the test specimens the axial and lateral deformations were determined with displacement transducers and a circumferential extensometer, respectively. A test specimen to determine the compressive strength is shown in Figure 1 (left). Figure 1 (right) illustrates the determined stress-strain curves of the calcium silicate units (top right) and of the autoclaved aerated concrete units (down right).

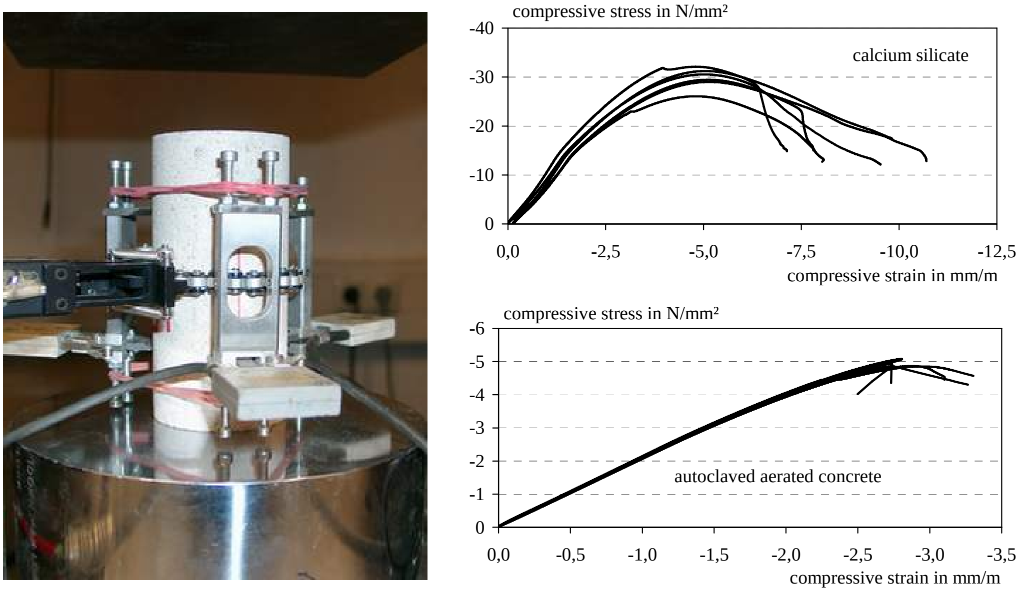


Figure 1. Compression tests on CS and AAC cylinders:
test setup and compressive stress-strain curves

## Tensile tests on cylinders

The load-deformation behaviour of the unit material under tensile load was investigated on cylinders (CS: ∅ = 50 mm, l = 100 mm; AAC: ∅ = 100 mm, l = 200 mm) drilled from the units in the direction of the unit length. The load introduction was made by steel plates flexibly jointed and attached to the testing machine as well as glued onto to the test specimens, see Figure 2 (left). The load-dependent deformations were determined with displacement transducers DD1 (measuring length 50 mm). The determined stress-strain curves for calcium silicate are illustrated in Figure 2 (top right) and for autoclaved aerated concrete in Figure 2 (down right).

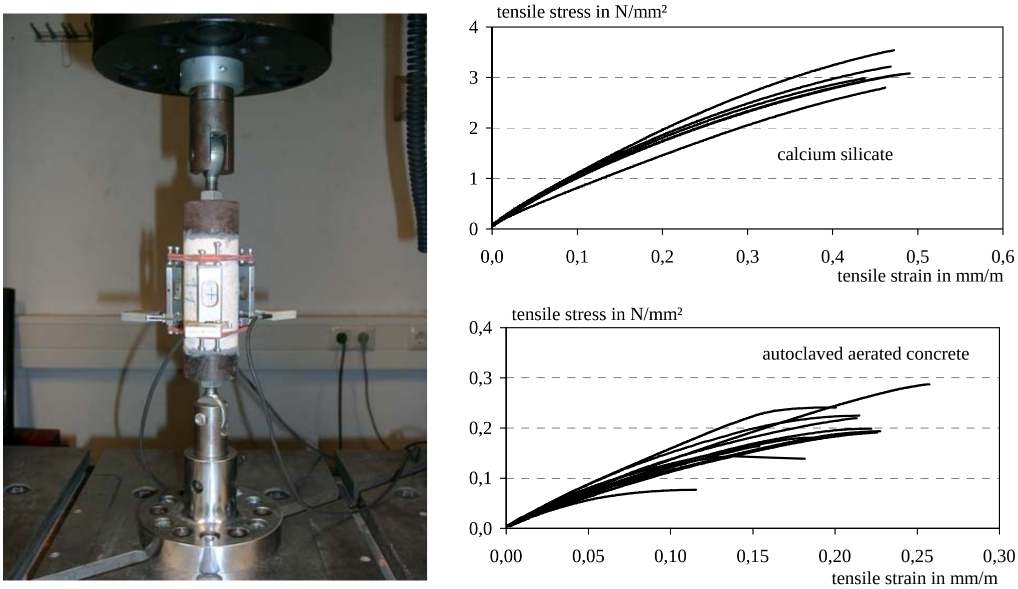


Figure 2. Tensile tests on CS and AAC cylinders:
test setup and tensile stress-strain curves

The test results of the tensile tests on AAC cylinders were comparatively small with regard to previous results found in literature. Therefore, further tests have to be conducted.

## Flexural tests on prisms

To be able to determine the post-failure behaviour of the calcium silicate material and the autoclaved aerated concrete under tensile load, deformation-controlled three-point bending tests (span 200 mm) were carried out on unnotched and notched prisms ($220 \cdot 40 \cdot 40$ mm³) taken in the direction of the masonry unit length. The respective test setup is presented in Figure 3 (left). The load-deflection curves determined on notched prisms are illustrated in Figure 3 (right).

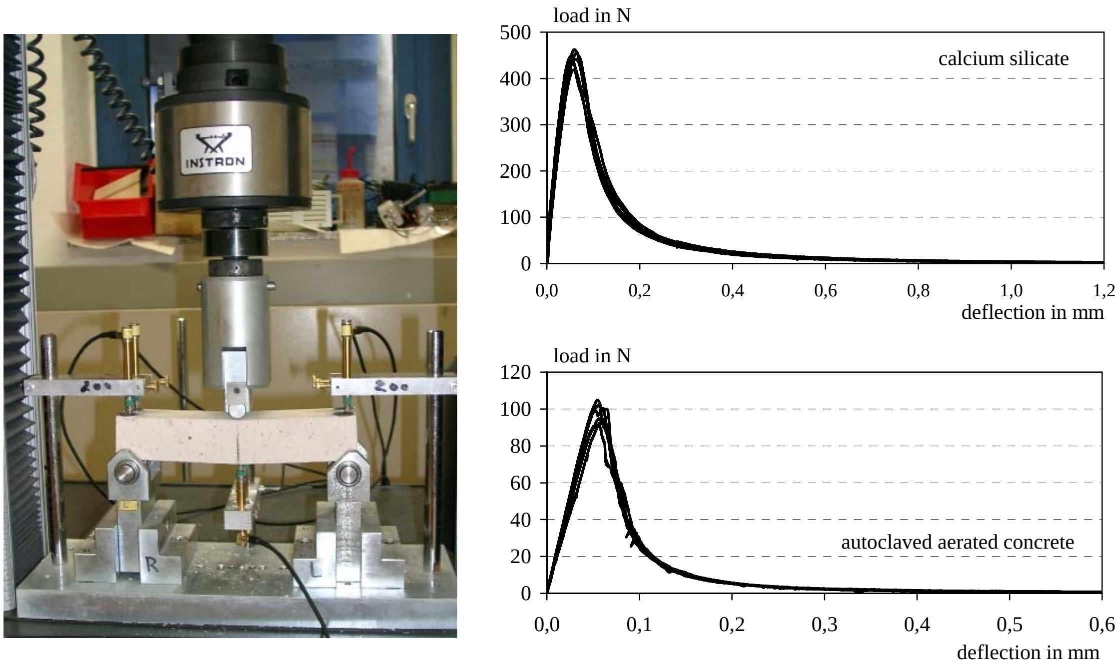


Figure 3. Three-point bending tests:
test setup, load–deflection curve of 10 mm notched prisms

All results of the small-size specimen tests on masonry unit material are compiled in Table 2.

Table 2. Properties of the unit material (mean values)

| Test | Parameter | | Unit type | |
|---|---|---|---|---|
| | | | CS | AAC |
| **Compression tests** | | | | |
| cylinder | compressive strength | $f_{c,cyl}$ [N/mm²] | 30.5 | 4.9 |
| | modulus of elasticity | $E_{33c,cyl}$ [N/mm²] | 9300 | 2000 |
| | Poisson's ratio | $\nu_{33,cyl}$ [-] | 0.12 | 0.11 |
| **Tension tests** | | | | |
| cylinder | tensile strength | $f_{t,cyl}$ [N/mm²] | 3.1 | 0.20 |
| | modulus of elasticity | $E_{33t,cyl}$ [N/mm²] | 10500 | 1600 |
| **Flexural tests** | | | | |
| notched prisms | net flexural strength | $f_{fl,net}$ [N/mm²] | 3.5 | 0.78 |
| | fracture energy | $G_F$ [N/m] | 50.3 | 9.8 |
| unnotched prisms | | | | |
| | flexural strength | $f_{fl}$ [N/mm²] | 4.7 | 0.93 |

## PROPERTIES OF THE MORTAR

To characterise the mortar properties, at first the hardened mortar characteristic values like flexural tensile strength $f_{fl}$ and compressive strength $f_{c,m,DIN}$ were determined according to the European Standard DIN EN 1015-11. The determination of the modulus of elasticity $E_{33c}$ and the Poisson's ratio $\nu_{33}$ on four large-size prisms (100 · 100 · 200 mm³) of each mix M1.1, M1.2 and M2.1 was made according to the German Standard DIN18555-4. These mixes were also used to manufacture the masonry pillars. The results of the tests are displayed in Table 3.

Table 3. Properties of the mortar (mean values)

| Test | Parameter | | Mortar type | | | |
|---|---|---|---|---|---|---|
| | | | M2.5 | | M10 | |
| | | | M1.1 | M1.2 | M2.1 | M2.2 |
| **Compression and flexural tests** | | | | | | |
| standard prisms | compressive strength | $f_{c,m,DIN}$ [N/mm²] | 2.7 | 2.6 | 15.2 | 22.7 |
| (160 · 40 · 40 mm³) | flexural strength | $f_{fl}$ [N/mm²] | 1.2 | 1.2 | 3.5 | 5.0 |
| **Compression tests** | | | | | | |
| large prisms | modulus of elasticity | $E_{33c}$ [N/mm²] | 4600 | 5300 | 13800 | - |
| (100 · 100 · 200 mm³) | Poisson's ratio | $\nu_{33}$ [-] | 0.19 | 0.16 | 0.19 | - |

Apart from the tests on the standard prisms hardened in the steel formworks also the material behaviour of the mortar after contact with the masonry unit was investigated to be able to investigate the influence of the different absorption properties of the respective unit types on the compressive strength and the deformation behaviour of the masonry pillars. To this end 2-unit specimens were manufactured additionally from each material combination according to Table 1. Parallel to the tests on the pillars, cubic prisms with the dimensions of $50 \cdot t_b \cdot 50$ ($t_b$ = joint thickness) to determine the joint compressive strength $f_{c,m,j}$ according to the German Standard DIN18555-9, (method III) and an oblong prism ($100 \cdot 50 \cdot t_b$ $mm^3$) to determine the dynamic modulus of elasticity were taken from each joint of these 2-unit specimens and tested.

It became obvious that the behaviour of the mortar in the joint very strongly deviates from the values determined on the standard prisms not only regarding the compressive strength but also with regards to the deformation behaviour. A comparison of the joint compressive strength $f_{c,m,j}$ with the mortar compressive strength $f_{c,m,DIN}$ determined on the standard prism is illustrated in Figure 4 (left) for both applied joint thicknesses. The ratio values of the dynamic modulus of elasticity from the joint and the static modulus of elasticity determined on large-size prisms $E_{dyn,j}$ / $E_{33,DIN}$ are shown in Figure 4 (right).

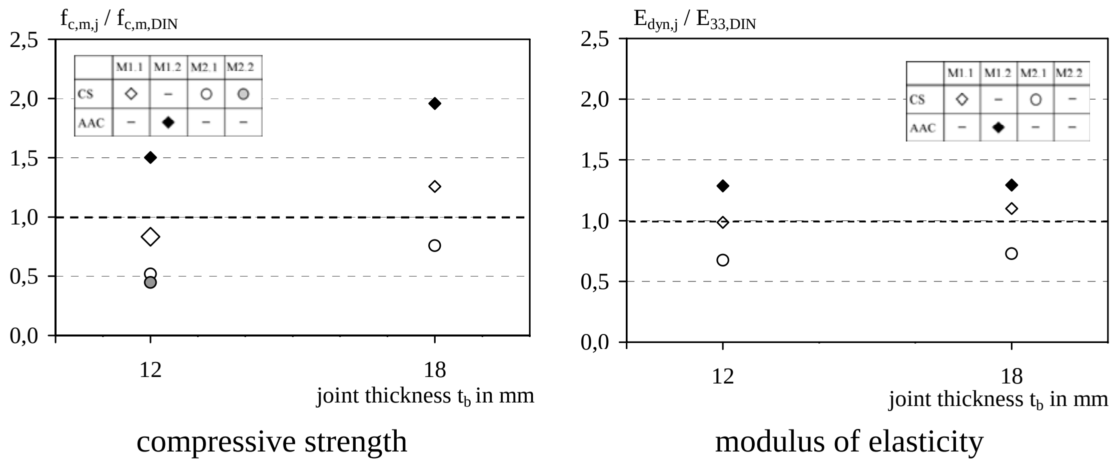


Figure 4. Tests on the mortar:
ratio values $f_{c,m,j}$ / $f_{c,m,DIN}$ and $E_{dyn,j}$ / $E_{33,DIN}$

## PROPERTIES OF THE MASONRY PILLARS

From the materials previously described, altogether 36 masonry pillars were manufactured with the unit-mortar combinations and the different joint thicknesses listed in Table 1. Apart from the mere determination of the compressive strength, here the deformation behaviour of the masonry pillars was of special interest. Therefore, in addition to the axial (L1-L4) and lateral strain (Q5-Q6) which are, as a rule, recorded at every pillar, numerous deformation measurement were conducted, amongst others with linear variable displacement transducers above the joint to determine the joint modulus of elasticity. In this process it turned out that the joint moduli of elasticity $E_{10,j}$ determined on the pillars amounted to only a fraction of the values determined on the standard prisms. The configuration of the measuring points for the deformation measurements on the pillar is schematically illustrated in Figure 5 (left).

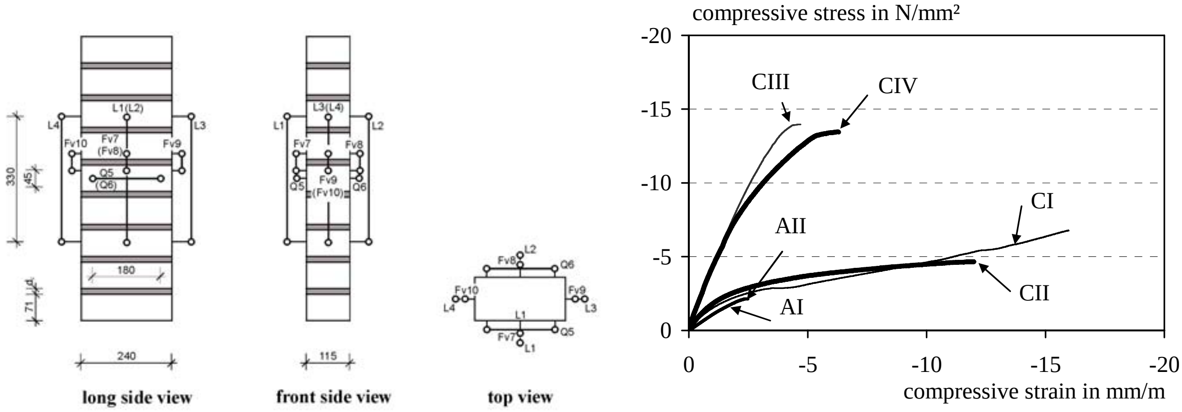


Figure 5. Compression tests on masonry pillars:
deformation measurements, experimental compressive stress-strain curves

In the compressive tests, the single test series showed a wide range of different global deformation behaviours. This is exemplarily shown in Figure 5 by means of one representative stress-strain curve for each single test series. Here, each curve results from the respective mean values of the axial measuring points L1 to L4. The stress-strain curves of the autoclaved aerated concrete pillars with the low-strength mortar (series AI and AII) featured a nearly linear gradient up to the fracture independent of the joint thickness. Only at a few test specimens the fracture became noticeable at about 80 % to 90 % of the maximum load when cracks occurred at the upper third of the pillar. Also the stress-strain curves of the calcium silicate pillars with the higher-strength mortar M10 featured a largely linear gradient especially with the smaller joint thickness (CIII). These pillars showed an utmost brittle failure, the crack formation started immediately before the failure of the pillar. The calcium silicate pillars with the low-strength mortar (CI and CII) failed, however, in an extremely ductile way at very high ultimate strains of about 15 mm/m, caused by an early breaking out of the mortar in the edge area and a slowly progressing damage of the mortar.

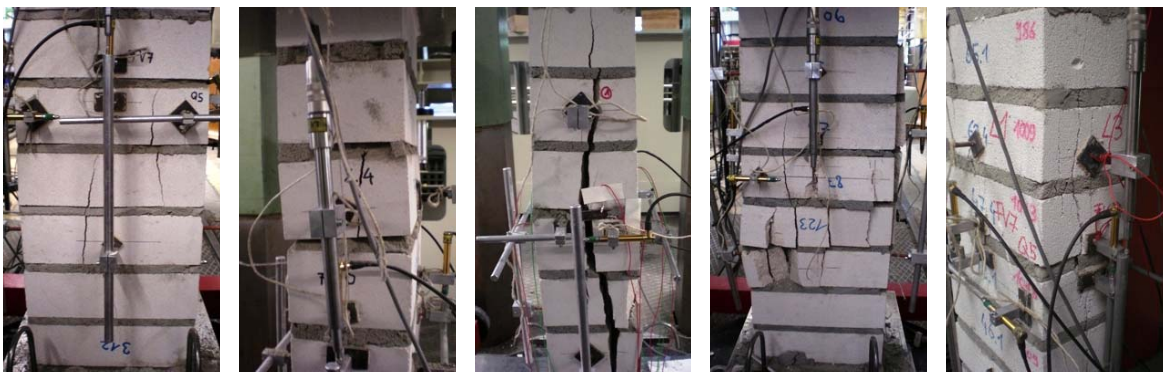

a) CI    b) CII    c) CIII, CIV    d) CIII, CIV    e) AI, AII

Figure 6. Compression tests on masonry pillars:
fracture pattern (exemplary)

The ratio values of the pillar compressive strength to the joint compressive strength were always lower at the test series with a joint thickness of 18 mm than at the thinner joints due to the higher lateral deformability of the mortar. The large difference between unit compressive strength and joint compressive strength at the series CI and CII led to a failure pattern which was characterised by a significant damage of the mortar, see Figure 6a) and b). Especially at the series CII, the larger joint thickness of 18 mm entailed that, as a rule, the units featured no

cracks at all. The series CIII and CIV presumably failed by exceeding the lateral tensile strength of the unit. As can be seen in Figures 6c) and d), at these series several partially wide cracks could form in the unit due to the better bond. The series AI and AII featured unit compressive strengths which ranged below the joint compressive strength. This led to a mostly abrupt failure with numerous thin cracks distributed over the unit, see Figure 6e). Here, the pillar compressive strength was presumably not decisively determined by the transverse tensile stresses but by an exceeding of the biaxial compressive strength of the masonry unit.

## THEORETICAL INVESTIGATIONS

With the material parameters previously determined in tests, the compressive tests on the masonry pillars were numerically simulated with the Finite Elements Programme DIANA. In doing so, the plasticity model according to Drucker-Prager in combination with the smeared crack model were taken as a basis to determine the failure in the tensile area. The friction angle according to Drucker-Prager was analytically determined for the units from the uniaxial strengths. According to Purtak (2001), the Drucker-Prager model can also be used to describe the yield strength of the mortar. On the basis of the test data in Bierwirth (1995), a friction angle of 20° had been derived. Additionally, the tests were simulated with a varying friction angle to closer investigate its influence on the stress distribution in the mortar. As material parameters of the mortar, the actual characteristics, i. e. the values determined on the mortar in contact with the unit, were applied. In comparison, simulations with the mechanical properties determined according to the mortar standard DIN EN 1015-11 were conducted.

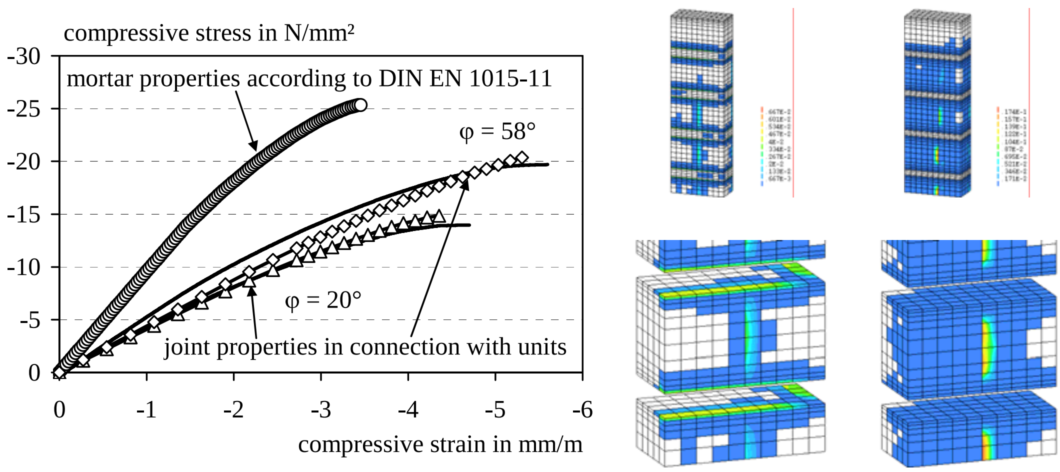


CIII CIV AI

Figure 7. Numerical simulations on masonry pillars:
comparison between experimental and numerical compressive stress-strain curves
numerical fracture pattern (exemplary)

Figure 7 (left) exemplarily shows a comparison of the experimentally determined stress-strain curves with the numerically calculated stress-strain curves for the test series CIII. It can be discerned that the consideration of the joint modulus of elasticity and the joint compressive strength normally led to a good correlation of the test results with the results of the numerical simulation. The deviations between the mean values of the experimentally determined and the numerically calculated stress-strain curves are from 1% to at maximum 11% and lay within the range of the scattering of the test data. The consideration of the mechanical properties

determined according to the mortar standard, however, led to significantly overestimated values of the stiffness and the load bearing capacity. Furthermore, Figure 7 (medium and right) illustrates two chosen crack patterns from the simulations of the series CIV and AI. Also the different crack patterns could be depicted correctly, cf. Figure 6. While in series CIV the cracks occurred as single wide cracks on the longitudinal side in the outer third and on the front side in the middle, numerous fine cracks were distributed over the entire unit at the series AI. These results correspond very well with the observations in the test.

## SUMMARY AND OUTLOOK

The masonry compressive strength depends on a multitude of influences. With the objective to predetermine the masonry compressive strength based on theoretical calculations taking into account all influences, extensive experimental tests on masonry pillars were carried out. Within the scope of these tests, numerous deformation measurements were conducted. Furthermore, all mechanical properties of the materials used were determined in parallel investigations. It was shown that the behaviour of the mortar in the joint is strongly affected by the water suction, not only regarding the compressive strength, but particularly in terms of joint deformations. Afterwards, the compressive tests on masonry pillars were numerically simulated with FEM. Therefore, the previously determined material properties were used. The global structural and deformational behaviour of the masonry pillars was accurately depicted by the simulation. The crack distribution, which is strongly affected by the respective unit-mortar combination, was also described appropriately. The consideration of the mechanical properties of the mortar inside the joint - instead of the mechanical properties determined according to the mortar standard - led to a considerable increase in accuracy of the numerical simulation. In the next steps of the project more unit-mortar combinations will be investigated and the numerical model modified for a more accurate damage analysis of masonry walls under compression.

## REFERENCES

Bierwirth, H.; Stöckl, S.; Kupfer, H.: Dreiachsige Druckversuche an Mörtelproben aus Lagefugen von Mauerwerk. München: Technische Universität, Institut für Tragwerksbau, Lehrstuhl für Massivbau, 1995. - DFG-Forschungsbericht, Nr. Ku 239/74-1 und 74/2

Hilsdorf, H.K.: Untersuchungen über die Grundlagen der Mauerwerksfestigkeit. München: Materialprüfungsamt für das Bauwesen der Technischen Universität München, 1965. - Bericht Nr. 40

Mann, W.: Druckfestigkeit von Mauerwerk ; Eine Statistische Auswertung von Versuchsergebnissen in geschlossener Darstellung mit Hilfe von Potenzfunktionen. Berlin: Ernst & Sohn, 1983 - In: Mauerwerkskalender 8 (1983), S. 687-699

Metje, W.-R.: Zum Einfluß des Feuchtigkeitszustandes der Steine auf das Trag- und Verformungsverhalten von Mauerwerk. Hannover, Technische Universität, Dissertation, 1983

Riechers, H.-J.: Ein neues Modell zur Beschreibung der Festigkeitsentwicklung von Mauermörtel in der Fuge: In: Schriftenreihe Aachener Beiträge zur Bauforschung, Institut für Bauforschung der RWTH Aachen (2000), Nr. 10, Dissertation

Purtak, F.: Tragfähigkeit von schlankem Quadermauerwerk aus Naturstein. Technische Universität Dresden, Fakultät Architektur, Dissertation, 2001